ISSN 2472-1972

Ablation of Oxytocin Neurons Causes a Deficit in Cold Stress Response

Dong Xi,[1] Caela Long,[1] Meizan Lai,[1] Alex Casella,[1] Lauren O'Lear,[1] Bassil Kublaoui,[1,2]* and Jeffrey D. Roizen[1,2]*

[1]Division of Endocrinology and Diabetes, The Children's Hospital of Philadelphia, Philadelphia, Pennsylvania 19104; and [2]University of Pennsylvania Perelman School of Medicine, Philadelphia, Pennsylvania 19104

*These authors are co-last authors.

The paraventricular nucleus (PVN) is a critical locus of energy balance control. Three sets of neurons in the PVN are involved in regulating energy balance: oxytocin-expressing neurons (OXT-neurons), thyrotropin-releasing hormone–expressing neurons, and corticotrophin-releasing hormone–expressing neurons. To examine the role of OXT-neurons in energy balance, we ablated these neurons in mice by injecting diphtheria toxin into mice possessing both the oxytocin promoter driving cre expression and a cre-inducible diphtheria toxin receptor. Immunohistochemistry and real-time reverse transcriptase polymerase chain reaction confirmed that this injection caused a significant decrease in PVN OXT-neurons and OXT-mRNA abundance. OXT-neuron ablation did not alter food intake, weight, or energy expenditure at room temperature on either chow or a high-fat diet. To further characterize OXT-neuron–ablated mice, we examined their response to 1) intraperitoneal cholecystokinin (CCK) injection and 2) thermogenic stress. OXT-neuron–ablated mice had a blunted decrease in feeding response to CCK. When exposed to the extreme cold (4°C) for 3 hours, OXT-neuron–ablated mice had significant decreases in both rectal and brown adipose tissue temperature relative to controls, which was rescued by OXT treatment. Thermographic imaging revealed that OXT-neuron–ablated mice had increased body surface temperature. Thus, we report that OXT-neuron ablation shows no role for OXT-neurons in energy homeostasis at neutral temperature but reveals a heretofore unappreciated role for OXT-neurons and oxytocin specifically in regulating the thermogenic stress response.

Freeform/Key Words: obesity, hypothalamus, oxytocin, cold stress, energy expenditure

Oxytocin (OXT) signaling deficits are implicated in the altered feeding behavior of several obesity-associated syndromes [1, 2]. However, the specific role of OXT-expressing neurons in energy balance regulation remains incompletely understood. OXT is synthesized centrally by cells in the paraventricular nucleus (PVN) and the supraoptic nucleus (SON) [3] but is released primarily from OXT-neurons in the PVN [4]. The PVN plays a critical role in control of energy balance [5]. Thus, OXT-neurons within the PVN have been the primary focus in determining the role of OXT in energy balance. Our previous work has shown decreases in PVN OXT-neuron number in a mouse model of hyperphagic monogenic obesity, *Single minded 1* (Sim1) haploinsufficiency [2]. We have also shown that intracerebral injection of oxytocin in Sim1-haploinsufficient mice rescues their phenotype of hyperphagic obesity. Further characterization of OXT in energy balance implicates OXT as an anorectic molecule primarily involved in limitation of meal size or intake of sweet solutions or carbohydrates

Abbreviations: ANOVA, analysis of variance; AVP, arginine vasopressin; BAT, brown adipose tissue; CCK, cholecystokinin; CRH, corticotropin-releasing hormone; ddPCR, droplet digital polymerase chain reaction; DT, diphtheria toxin; DTR, diphtheria toxin receptor; iDTR, inducible diphtheria toxin receptor; IP, intraperitoneal; NYS, solitary nucleus; OXT, oxytocin; PBS, phosphate-buffered saline; PCR, polymerase chain reaction; PVN, paraventricular nucleus; SON, supraoptic nucleus; TRH, thyrotropin-releasing hormone; UCP1, uncoupling protein 1.

Received 11 March 2017
Accepted 7 July 2017
First Published Online 12 July 2017

[6–11]. This role appears to be mediated by potentiation of the effects of the satiety-inducing peptide cholecystokinin (CCK) through OXT release at the solitary nucleus (NTS) [12]. This work seems to identify a critical role for oxytocin in feeding; however, other studies complicate this picture. Initial work on OXT knockout mice described no metabolic phenotype, whereas recent work has reported late-onset obesity in oxytocin receptor–deficient mice [13] as well as OXT knockout mice [14]. This obesity appears to be the result of altered energy expenditure rather than altered food intake. Thus, in addition to possibly controlling an aspect of carbohydrate appetite, OXT may be involved in regulation of body composition and energy expenditure [14, 15].

Another group has used a similar approach to oxytocin ablation in adult mice as our group and characterized aspects of altered metabolism in OXT-neuron–ablated mice [15]. They observed a sex-dependent increase in sensitivity of OXT-neuron–ablated male mice to high-fat diet–induced weight gain (independent of increased food intake), increased body fat composition, and decreased sensitivity to leptin injection–induced anorexia 4 and 24 hours after injection. Therefore, the observed increase in weight gain is a consequence of an attenuated metabolism—due to the high-fat diet—and the disrupted energy balance in the PVN.

The role of oxytocin in energy balance has been investigated using an oxytocin agonist and a rat model of CCK-mediated anorexia and leptin-mediated decrease in meal size [7, 12]. PVN OXT leptin–activated neurons project to the NTS, and oxytocin receptor antagonist injections into the fourth ventricle attenuated the anorectic effect of leptin. In contrast to the chemical ablation experiments previously described, peripheral administration of oxytocin suppressed food intake [16], and third-ventricle administration of an oxytocin antagonist inhibited both leptin-mediated decrease in meal size and CCK-mediated decrease in food intake. Thus, oxytocin may have effects that both decrease food intake and increase energy expenditure.

Diet-induced thermogenesis is a critical pathway implicated in the control of energy balance. Postmeal body temperature increase is dependent on signaling through the β1, β2, and β3 adrenergic receptors to increase heat generation [17, 18] via uncoupling protein 1 (UCP1) action in brown fat. Cold-induced thermogenesis utilizes a similar final pathway but is thought to be controlled upstream of β-adrenergic receptor activation via different mechanisms [19, 20]. For instance, obese individuals have a decreased postmeal increase in body temperature relative to lean individuals [20], and this work suggests that regulation of cold-induced thermogenesis may have more in common with diet-induced thermogenesis than previously thought.

To further characterize the role of OXT-neurons in energy balance regulation, we characterized several aspects of metabolism in OXT-neuron–ablated mice: leptin-induced satiation signaling in the PVN, the physiological response of OXT-neuron–ablated mice to thermogenic stress at 4°C, the abundance of UCP1 mRNA transcripts brown fat of OXT-neuron–ablated mice, and exogenous OT treatment of cold stress. We hypothesize that OXT-neuron–ablated mice will have deficits in energy expenditure regulation, specifically in the context of thermogenesis. Our results demonstrate a role for OXT-neurons and oxytocin in the response to thermogenic stress.

1. Materials and Methods

A. Experimental Animals and Genotyping

All procedures were carried out in accordance with the National Institutes of Health Guidelines on the Care and Use of Animals and approved by the Children's Hospital of Philadelphia Institutional Animal Care and Use Committee (Protocol #2009-10-895).

Oxytocin-Ires cre mice were obtained from Dr. Bradford B. Lowell [15]. Inducible diphtheria toxin receptor (iDTR) mice, which express inducible diphtheria toxin receptor (DTR), were purchased from Jackson Laboratory (Bar Harbor, ME; stock #007900). OXTcreiDTR mice were generated by mating OXTcre mice with iDTR mice. iDTR-positive OXTcre negative littermates were used as controls.

Mice were housed at 20 to 24°C with a 12-hour light/dark cycle. Food and water were provided *ad libitum*. To achieve specific oxytocin neuron ablation, OXTcreiDTR mice around 6 weeks of age were injected intraperitoneally with diphtheria toxin (DT) [Sigma, St. Louis, MO; D-0564; 1.0 μg dissolved in phosphate-buffered saline (PBS)]. Control mice also received the same DT treatment.

All pups were genotyped using the following primer sequences: For Cre: Cre800, 5′-GCTGCCACGACCAAGTGACAGCAATG-3′; Cre1200, 5′- TAGTTATTCGGATCATCAGC-TACAC-3′; for iDTR: OL260: CTL 5′-CATACTGCATGTGTCTTGGTGGGCTGAGCC-3′; OL261: CTL 5′-GAATCCTGTGCAATACTCACCACTCCAGGC-3′.

B. Experimental Schedule

Mice were weaned at 3 weeks. Six-week-old mice (male and female) received an intraperitoneal (IP) injection of DT or vehicle (PBS) as described above and then were separated and fed with chow diet for 8 weeks. Body weight and food intake were monitored weekly. Energy expenditure was measured at 6 weeks after treatment with DT (12 weeks of age). After energy expenditure was measured, mice were used in studies on sucrose intake, response to systemic treatment with CCK, food choice, and response to cold exposure.

After mice were euthanized, neuronal ablation was confirmed by OXT immunofluorescence staining and real-time reverse transcriptase polymerase chain reaction, both performed as described before [21]. In brief, mice were euthanized and perfused with 4% paraformaldehyde. The hypothalamus and pituitary were dissected, and punch biopsies of the PVN or SON were taken. Total mRNA was isolated using RNAEasy (Qiagen, Germantown, MD) per manufacturer instructions. cDNA was synthesized using the iScript cDNA Synthesis kit. Duplex quantitative polymerase chain reaction (PCR) was performed using an ABI step-one plus real-time PCR system (Applied Biosystems, Foster City, CA) and Taqman assays for the following genes with β-actin (Applied Biosystems) or glyceraldehyde 3-phosphate dehydrogenase (Mm99999915-g1) as the control (the data shown are using actin as a control). Each quantitative PCR experiment was repeated using glyceraldehyde 3-phosphate dehydrogenase as the control. The results were similar overall and identical with respect to level of statistical significance. The following probes were used: OXT (Mm00726655 s1) and UCP1 (Mm01244861_m1). Real-time reverse transcriptase PCR results were confirmed by droplet digital PCR (ddPCR) using the same probes and master mix with the Bio-Rad QX100 ddPCR machine per manufacturer specifications. For ddPCR, all probes were used within the linear range of concentrations, and all results were similar overall and identical with respect to level of statistical significance.

C. Confirmation of DT OXT-Neuron Ablation

Mice were euthanized and perfused with 4% paraformaldehyde. Brains were harvested and sectioned into 30-μm sections for immunocytochemistry using a microtome (SM2000 R Sliding Microtome; Leica). Sections containing the PVN and NTS were targeted with the aid of the Franklin and Paxinos Brain Atlas. OXT-neurons were specifically targeted using a mouse anti-OXT primary antibody (RRID:AB_2157626) and goat anti-mouse secondary cy3-conjugated antibody (RRID:AB_10892840). Additionally, thyrotropin-releasing hormone (TRH), corticotropin-releasing hormone (CRH), and arginine vasopressin (AVP) neurons were stained to determine that DT treatment only ablated OTX-neurons. The primary antibodies raised in rabbit for TRH (RRID:AB_2665393; Eva Redei Laboratory Northwestern University, Chicago, IL), CRH (RRID:AB_171828), and AVP (RRID: AB_572219) were stained for with secondary antibody (goat anti-rabbit Dylight 488 conjugated; RID:AB_2556658).

D. Metabolic Characterization of Mice

Metabolic characterization of mice was performed as described previously [21]. Body weight and food intake were measured weekly on a chow diet. Energy expenditure was measured in a

Comprehensive Laboratory Animal Monitoring System from Columbus Instruments over a 24-hour period. Volume of oxygen and volume of carbon dioxide were normalized to body weight (n = 4 for each group).

E. CCK Treatment and Post-CCK C-Fos Immunohistochemistry

This study was performed on 14-week-old mice (8 weeks after DT injection). For food intake, each mouse served as its own control; the first night mice received IP injection of vehicle and were allowed *ad libitum* access to chow diet. Food intake was measured at 1, 2, and 4 hours after injection. After a 24-hour recovery period, mice were injected at the beginning of the dark cycle with 0.125 μg of CCK (SP3443; Abgent). Food intake was again measured at 1, 2, and 4 hours after injection. Brain sections were harvested in the same manner described above. Sections were incubated in primary antibody [rabbit anti–c-fos (RID:AB_2106765), 1:2000 diluted in 0.3% Triton-PBS] for 36 hours at 4°C and then in secondary antibody (goat anti-rabbit secondary Dylight 488–conjugated RRID:AB_2556658), 1:800 diluted in 0.3% Triton-PBS for 2 hours at room temperature. c-fos–positive neurons in PVN and NTS in OXTcreiDTR mice were counted and compared with iDTR mice. To avoid double counting, a 4 × 4 cm grid was used on printed images of sections acquired under 10× magnification. Additionally, costains for c-fos and TRH, CRH, AVP, and OXT neurons were conducted to specify which neuron subsets in the PVN were being activated by CCK. OXT-, TRH-, CRH-, and AVP-neuron staining were conducted as described above. However, for costains in which the primary antibody being stained for with c-fos was raised in rabbit (TRH, CRH, and AVP), mouse anti–c-fos primary antibody (RRID: AB_2665387) was used with Cy3-conjugated goat anti-mouse secondary antibody (RID: AB_10892840).

F. Sucrose Intake and Food Choice Experiments

This study was performed on 14-week-old mice (8 weeks after DT injection). These mice were subjected to food deprivation for 12 hours prior to the test and allowed *ad libitum* food access during the test. They had access to 20% sucrose solution (20 g sucrose dissolved in 100 mL; Sigma) and nonsucrose water. Solution intake was measured daily for 1 week. Mice were given a week to recover and then subjected to the food choice study. Mice were fed separate diets of chow (PicoLab Mouse Diet 20; Labdiet, Elkridge, MD) containing 3.75 kcal/g (10% fat) and high-fat diet (diet-induced obesity diet; 60 kcal% fat) (D12492; Research Diet, New Brunswick, NJ) for 1 week. Food intake and body weight were measured daily.

G. Cold Exposure Experiments

A temperature transponder (Model IPTT-300; Bio Medic Data Systems, Seaford, DE), calibrated per the manufacturer's instructions, was embedded between the scapulae of 14-week-old mice (8 weeks after DT injection). The transponders were injected into awake animals between the shoulder blades using a sterilized needle injector provided with the transponders. Brown adipose tissue (BAT) temperature was measured initially at room temperature. Mice were then placed at 4°C, and BAT temperature was measured 30 minutes and 1 hour later. Core temperature, energy expenditure, oxygen consumption, CO_2 production, metabolic rate, and total activity were measured. Core body temperature was measured using a rectal thermometer (model Temp10T; Oakton, Vernon Hills, IL) that was calibrated as per the manufacturer's instructions. Thermographic imaging was performed at room temperature and at the end of 3 hours of cold exposure. To control for possible stress, the effect of prior stress, and time of day, all measures were performed on controls and OXT-neuron–ablated mice in sets of pairs. Measures were performed each morning at 2 hours after lights on in the animal facility.

H. Oxytocin Treatment Experiment

Using the same methods as in the cold exposure experiment above, an Oakton temperature transponder was embedded between the scapula of 14-week-old mice, and core body temperature was measured using an Oakton rectal thermometer. BAT temperature and core body temperature were measured initially at room temperature and then again at 6 hours. Mice were divided into two groups (n = 3 for each group) and were examined on two consecutive days. One group received an oxytocin injection on day 1 and vehicle (saline) on day 2; the other group received vehicle injection on day 1 and oxytocin (Bachem, Torrance, CA) on day 2. Oxytocin was dissolved in saline containing 0.002% acetic acid. For acute treatments, mice were given a single IP injection of vehicle or 1.0 mg/kg oxytocin immediately prior to testing. Mice were then placed at 4°C, and BAT temperature and core temperature were measured 30 minutes and 1 hour later.

I. Data Analysis

All values are presented as mean ± standard error of the mean and represent data from a minimum of two repeated experiments (n = ≥3 for each experiment). Data were analyzed using Prism Software version 6 (GraphPad Software, San Diego, CA) or JMP version 10 (SAS Institute, Cary, NC). Means were compared using a two-tailed *t* test, with Welch's correction or repeated-measures two-way analysis of variance (ANOVA) with Sidak's posttests as appropriate. Temperature distributions were compared using a Kolmogorov–Smirnov test using R for MacOS (www.r-project.org, version 3.0.2). Differences were considered statistically significant at $P < 0.05$.

2. Results

A. Ablation of OXT Neurons Through DT Treatment

To assess the extent of OXT neuron ablation after DT treatment, immunofluorescence staining of OXT was performed in both iDTR and OXTcreiDTR mice [representative images are shown in Fig. 1(a)]. OXT-positive neurons in the PVN were counted and compared

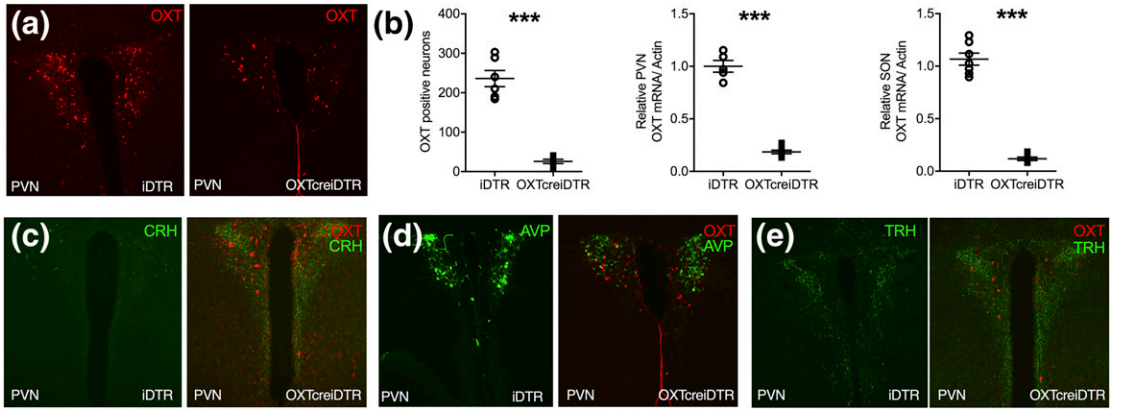

Figure 1. Confirmation of OXT neuron ablation. (a) Immunofluorescence staining with OXT antibody in PVN of iDTR (left) and OXTcreiDTR (right) mice. (b) Quantitation of OXT-positive cell number in the PVN (n = 3 for each group; ***$P < 0.01$), relative OXT mRNA abundance in the PVN in iDTR vs OXTcreiDTR mice by real-time PCR (n = 4 or 5 for each group; ***$P < 0.01$) and OXT mRNA abundance in the SON in iDTR vs OXTcreiDTR mice by real-time PCR (n = 4 or 5 for each group; ***$P < 0.01$). Immunofluorescence staining with CRH (c), AVP (d), and TRH (e) antibody in PVN of iDTR (left) and costained with OXT antibody in PVN of OXTcreiDTR (right) mice.

between genotypes. OXTcreiDTR mice displayed a significant ($P < 0.01$) reduction of OXT neurons in the PVN [Fig. 1(b)]. Concurrent OXT mRNA transcript abundance was decreased by >80% relative to iDTR mice in both the PVN and the SON [Fig. 1(b)]. These results are similar to those reported by others [15]. Additionally, there was not a significant difference in the number of CRH-, AVP-, or TRH-positive neurons in the PVN between iDTR unablated control mice (left) and OxtcreiDTR neuron–ablated mice (right) [Fig. 1(c) and 1(e), respectively]. Costaining for OXT and CRH, AVP, or TRH revealed a decrease in OXT-neurons in OxtcreiDTR neuron–ablated mice, whereas the number of CRH, AVP, or TRH neurons was not significantly decreased [Fig. 1(c)].

B. OXT Neuron Ablation Does Not Alter Food Intake and Energy Expenditure at Room Temperature

To examine the role of OXT-neurons in energy balance regulation, we compared body weight of male and female mice [Fig. 2(a) and 2(b)] respectively], food intake [Fig. 2(c) and 2(d)], and energy expenditure [Fig. 2(e) and 2(f)] on a chow diet between OXT-neuron–ablated mice and unablated control mice (OxtcreiDTR DT treated vs iDTR DT treated). No significant differences in body weight, caloric intake, or energy expenditure were observed between groups (Fig. 2). Other groups have reported body composition changes due to oxytocin in similar model systems [22], and our approach does not rule this possibility out. However, metabolic rate was also not significantly different between groups, suggesting that any differences in body composition, which would be expected to alter metabolic rate, are likely to be small. It is also possible that this negative result reflects that our OXT-neuron ablation was incomplete and that the lack of a phenotype here reflects residual OXT-neuron function.

C. OXT-Neuron Ablation Causes Increased Sucrose Solution Intake but Does Not Alter Food Preference

Previous work implicates OXT as having a role in intake of sucrose solution, namely that OXT-null mice ingest an increased amount of sucrose [6, 23]. To address the possibility that OXT-neurons are involved in limiting the intake of sucrose solution, we examined the intake of a 20% sucrose solution by OXT-neuron–ablated mice. We found that daily solution intake of OXTcreiDTR mice was significantly increased relative to intake in iDTR control mice (20.28 ± 0.72 vs 17.81 ± 0.90 mL; $P < 0.05$) [Fig. 3(a)], but there were no differences in plain water intake during this period. To examine the possibility that this altered limitation of sucrose intake would lead to a decreased preference for high-fat chow, we tested the preference of both groups of mice for normal chow and high-fat chow over 1 week. No differences in overall intake or in food preference were observed between groups [Fig. 3(b)]. Similarly, no differences on body weight change during this week were observed between groups (0.68 ± 0.22 g for iDTR vs 0.69 ± 0.19 for OXTcreiDTR) [Fig. 3(c)], consistent with the idea that OXT-neurons are less critical for regulation of fat intake than they are to regulation of carbohydrate intake.

D. OXT-Neuron Ablation Causes Blunted Anorexic Response to CCK

The current model for oxytocin neuron–mediated anorexia, elucidated in rats, is that leptin signaling is mediated via activation of PVN OXT neurons, with output from these neurons ultimately suppressing food intake by acting on CCK-responsive neurons in the NTS. Furthermore, CCK injection induces c-Fos in NTS and PVN neurons. To determine if OXT-neurons are necessary for CCK-mediated anorexia, we injected these mice with CCK during the dark cycle and measured food intake 1, 2, and 4 hours after chow intake. As expected, relative to vehicle-injected mice, CCK-injected iDTR mice had significantly decreased ($P < 0.05$, two-way ANOVA) chow intake at 2 and 4 hours [Fig. 4(a)], at 2 hours intake decreased by 65% of vehicle-injected ($P < 0.001$, Sidak's correction for multiple comparisons), and at

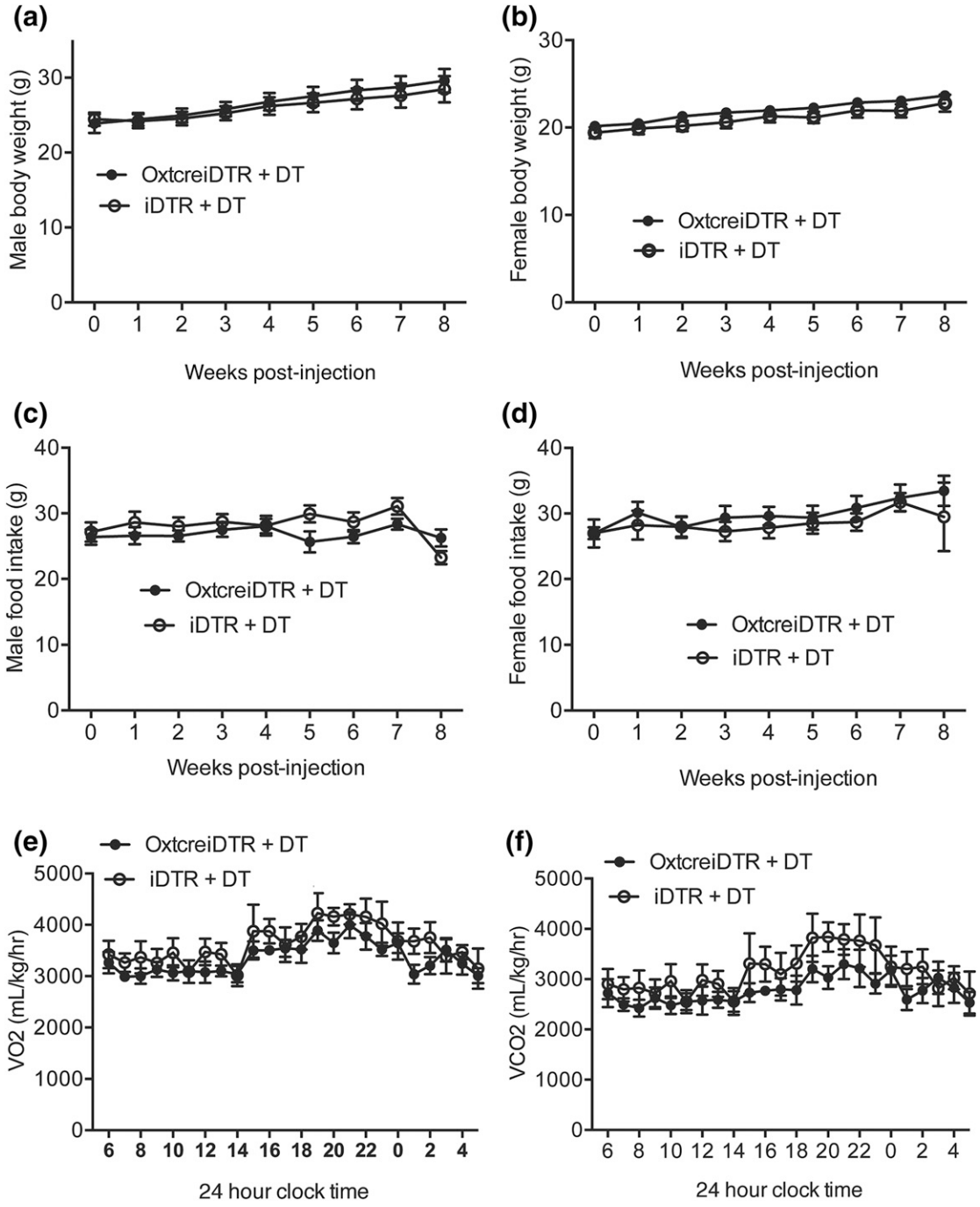

Figure 2. OXT neuron ablation did not have an effect on food intake and energy expenditure on a chow diet. Body weight and food intake of male (a, c), and female (b, d) iDTR vs OXTcreiDTR mice. DT (1 μg) was injected intraperitoneally at week 0 (6 weeks of age). Body weight and food intake were measured weekly on a chow diet (n = 8 to 10 per group). Energy expenditure was measured in CLAMS cages over a 24-hour period. VO_2 (e) and VCO_2 (f) were normalized to body weight (n = 4 for each group). Overall group means and then means at each time point or condition were compared by a *t* test or ANOVA as appropriate. Error bars indicate standard error of the mean. VO_2, volume of oxygen; VCO_2, volume of carbon dioxide.

4 hours intake decreased by 57% of vehicle-injected ($P < 0.0001$, Sidak's correction for multiple comparisons). In OXTcreiDTR mice, CCK injection did not significantly decrease chow intake overall or at any time point.

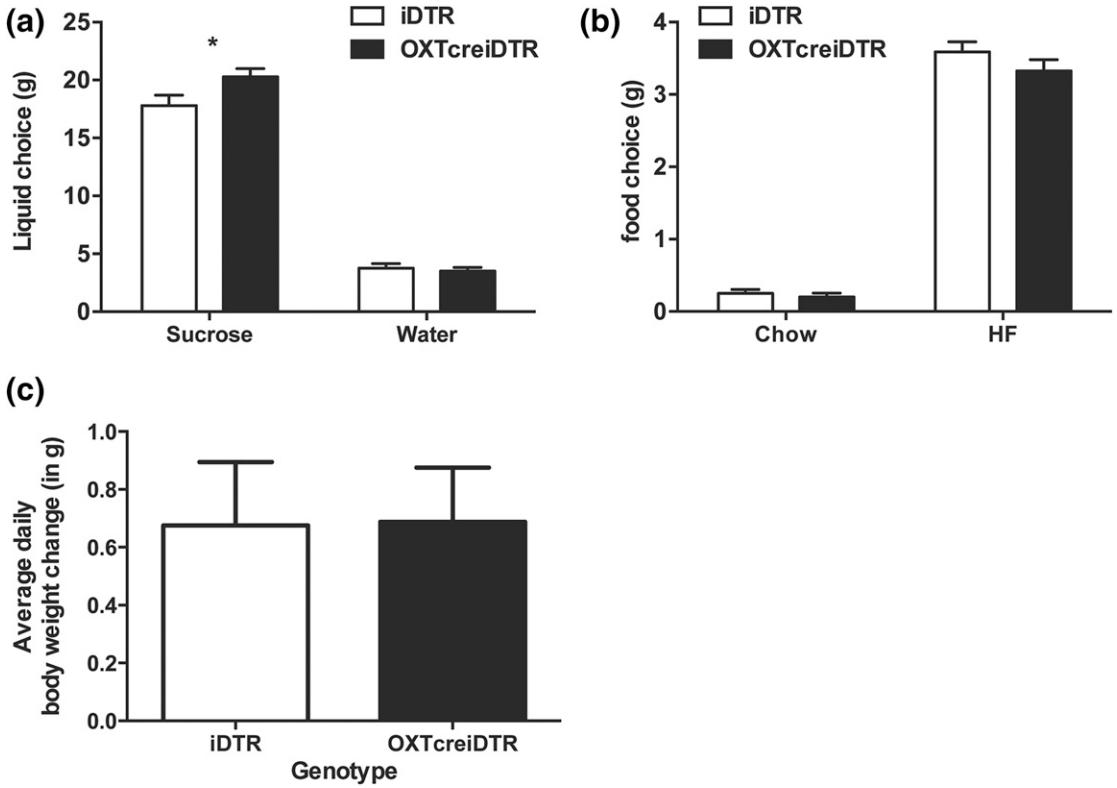

Figure 3. Male mice with OXT neuron ablation have decreased anorexic response to CCK injection and decreased limitation of sweet liquid intake but no alteration in food preference. (a) Sucrose liquid intake was measured for 1 week (n = 4 for each group; $P < 0.05$) (weight-adjusted intake was also significant; data not shown). (b) Mice were given a choice of separate diets of normal chow and high-fat chow (n = 4 for each group). No differences in overall intake or food preference were observed between groups, either unadjusted or adjusted for animal weight. (c) Body weight change was measured for 1 week and averaged. No significant differences were noted between groups. Error bars indicate standard error of the mean.

E. OXTcreiDTR Mice Have Blunted PVN Activation to CCK Injection

To explore the cellular mechanism underlying the blunted anorexic response to CCK, we performed immunofluorescence staining of c-Fos at 4 hours after CCK injection to examine the activation of PVN and NTS neurons [Fig. 4(b) and 4(d) respectively]. Compared with iDTR control mice, the number of c-fos–positive neurons in the PVN in OXTcreiDTR mice after CCK injection was significantly decreased (41% of iDTR mean; $P < 0.05$). However, these two genotypes did not have significant differences in the number of c-fos–positive neurons at baseline [Fig. 4(c)]. In the NTS, no significant differences in c-fos–immunoreactive neurons were observed (94% of iDTR mean) [Fig. 4(d).] Additionally, costaining was conducted for c-fos and OT, AVP, CRH, and TRH in iDTR mice to determine which specific subset(s) of neurons in the PVN are being activated. OXT-neurons were the only subset of neurons that showed colocalization with c-fos staining 4 hours after CCK injection [Fig. 4(e)].

F. OXT Neurons are Critical for Cold-Induced Thermogenesis in Male Mice

Other work has shown that OXT neuron ablation leads to weight gain in male mice but not in female mice on high-fat chow due to decreased energy expenditure [15]. We hypothesized that this weight gain may be due in part to deficits in thermogenesis and that these deficits might extend beyond diet-induced thermogenesis to include cold-induced thermogenesis. To examine the role of OXT-neurons in cold-induced thermogenesis, we exposed our mice to

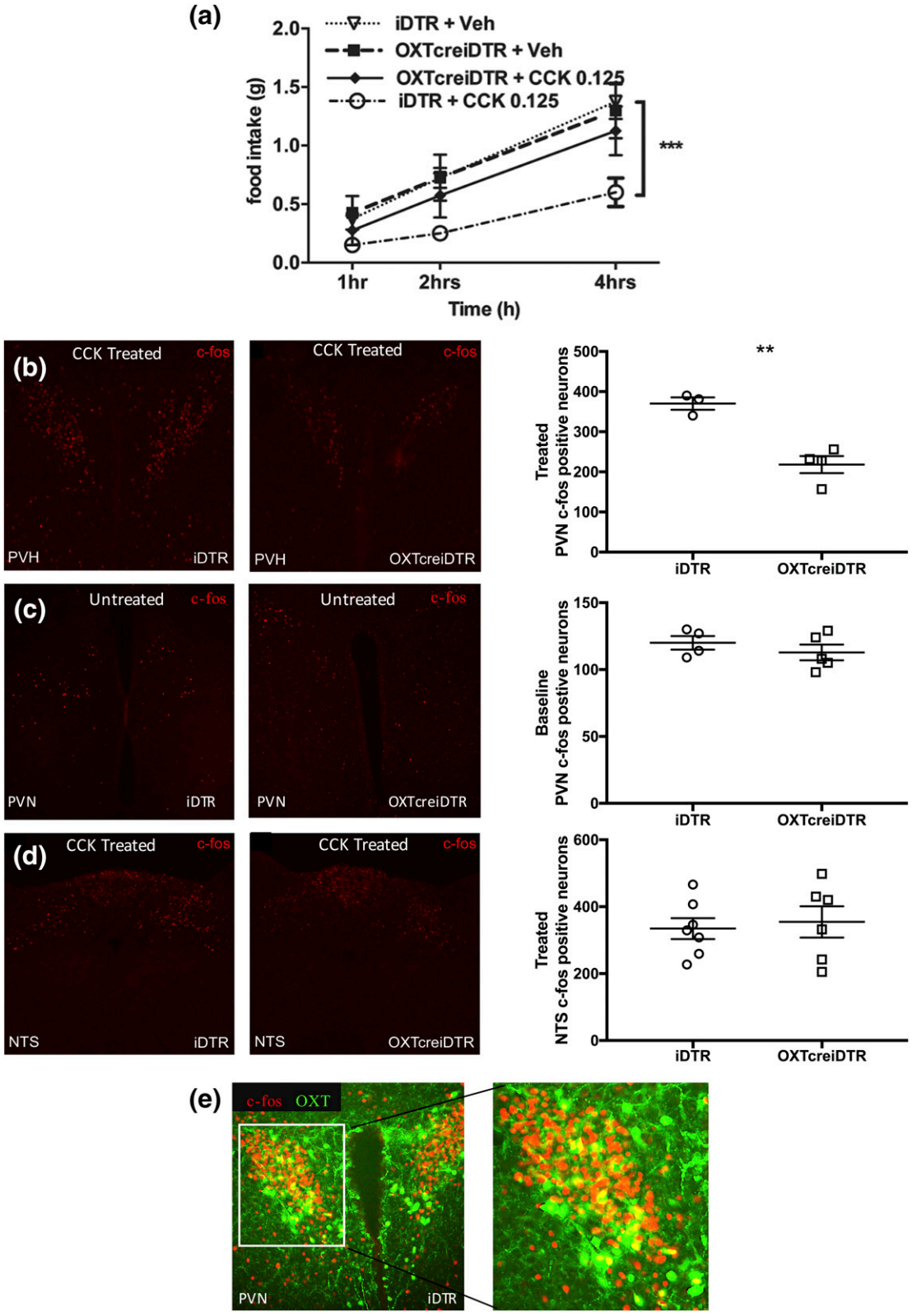

Figure 4. Male OXT-neuron–ablated mice have decreased activation of PVN neurons after CCK injection. (a) OXTcreiDTR mice have decreased anorexic response to CCK injection (**$P < 0.01$; ***$P < 0.001$). (b–d) Quantitation of c-fos–positive cell number to the right of staining. Immunofluorescence staining with c-fos antibody in PVN (b) and NTS (d) of iDTR

and OXTcreiDTR mice 4 hours after CCK injection. (c) Staining with c-fos antibody in PVN of iDTR and OXTcreiDTR mice at baseline (no CCK treatment). (e) Costaining for c-fos with OXT-positive neurons in the PVN of iDTR mice 4 hours after CCK injection. Error bars indicate standard error of the mean.

extreme cold (4°C) and monitored their BAT temperature, their core temperature, and their surface temperature. At room temperature, the BAT temperature of OXT-neuron–ablated mice is not significantly different from that in iDTR mice (37.05 ± 0.28 vs 37.15 ± 0.14) [Fig. 5(a)]. During cold exposure, BAT temperature increased in both groups; however, the BAT temperature increase in iDTR mice was significantly greater than that in the OXT-neuron–ablated mice (at 30 minutes, 1.53 ± 0.23°C vs 0.68 ± 0.09°C, $P < 0.01$; at 1 hour, 1.35 ± 0.26°C vs 0.65 ± 0.09°C; $P < 0.05$) [Fig. 5(b)]. During the same exposure, both sets of mice exhibited a slight decrease in their core body temperature. The decrease in core body temperature was not significant in iDTR mice, whereas this decrease was significant in OXT-neuron–ablated mice ($P > 0.01$) [Fig. 5(c)]. Using thermographic imaging [representative images are shown in Fig. 5(d)], we compared the heat distribution at the skin at the end of the cold exposure between groups [averaged temperature distribution curves for male mice are shown in Fig. 5(e)]. This comparison revealed an increase in surface body temperature in OXTcreiDTR mice relative to iDTR mice (group distributions significantly different with $P < 0.001$ by Kolmogorov–Smirnov test).

G. Male OXT-Neuron–Ablated Mice Have Normal Capacity for Thermogenesis in Response to Oxytocin

To determine if OXT-neurons play only an acute role in activating thermogenesis or if their intermittent activation (postmeal or in response to transient temperature changes) is critical to building the capacity for thermogenesis, we examined the relative abundance of UCP1 mRNA in the brown fat of OXT-neuron–ablated mice. There was no alteration in UCP1 mRNA in the brown fat of OXT-neuron–ablated mice (n = 7 for each) [Fig. 6(a)]. To determine if oxytocin treatment would alter BAT thermogenesis and adaptation to cold stress, we compared the BAT temperature and core temperature of OXT-neuron–ablated mice under cold stress with and without OXT treatment. The cold-stress–mediated decrease in BAT temperature (paired t test, $P < 0.01$; n = 6) [Fig. 6(b)] and core temperature ($P < 0.05$; n = 6 for each) [Fig. 6(c)] were dramatically attenuated by OXT pretreatment. By contrast, iDTR control mice subjected to the same treatment had no significant attenuation in their cold-stress–mediated decrease in BAT temperature or core temperature [Fig. 6(b) and 6(c)], suggesting that oxytocin pretreatment in OXT-neuron–ablated mice represents a rescue of function rather than a gain of function.

3. Discussion

Oxytocin signaling has been implicated in energy homeostasis, but the precise role of oxytocin remains a topic of debate. Initial investigations in mice using genetic approaches to examine the role of oxytocin in energy homeostasis gave negative results. This body of work was bedeviled by the likelihood that congenital lack of oxytocin signaling gave rise to developmental adjustments that compensated for the lack of oxytocin. In rats, the use of pharmacologic antagonists of the OXT receptor has revealed several roles for OXT in hypothalamic integration of acute [12] and chronic [7] signaling of organismal energy status. This work in rats has not been confirmed in mice. Recent work in mice has attempted several approaches to the problem of developmental compensation including the adult lesion of oxytocin neurons. Using this approach, we observed results that reproduce previous findings with respect to the role of oxytocin in energy homeostasis.

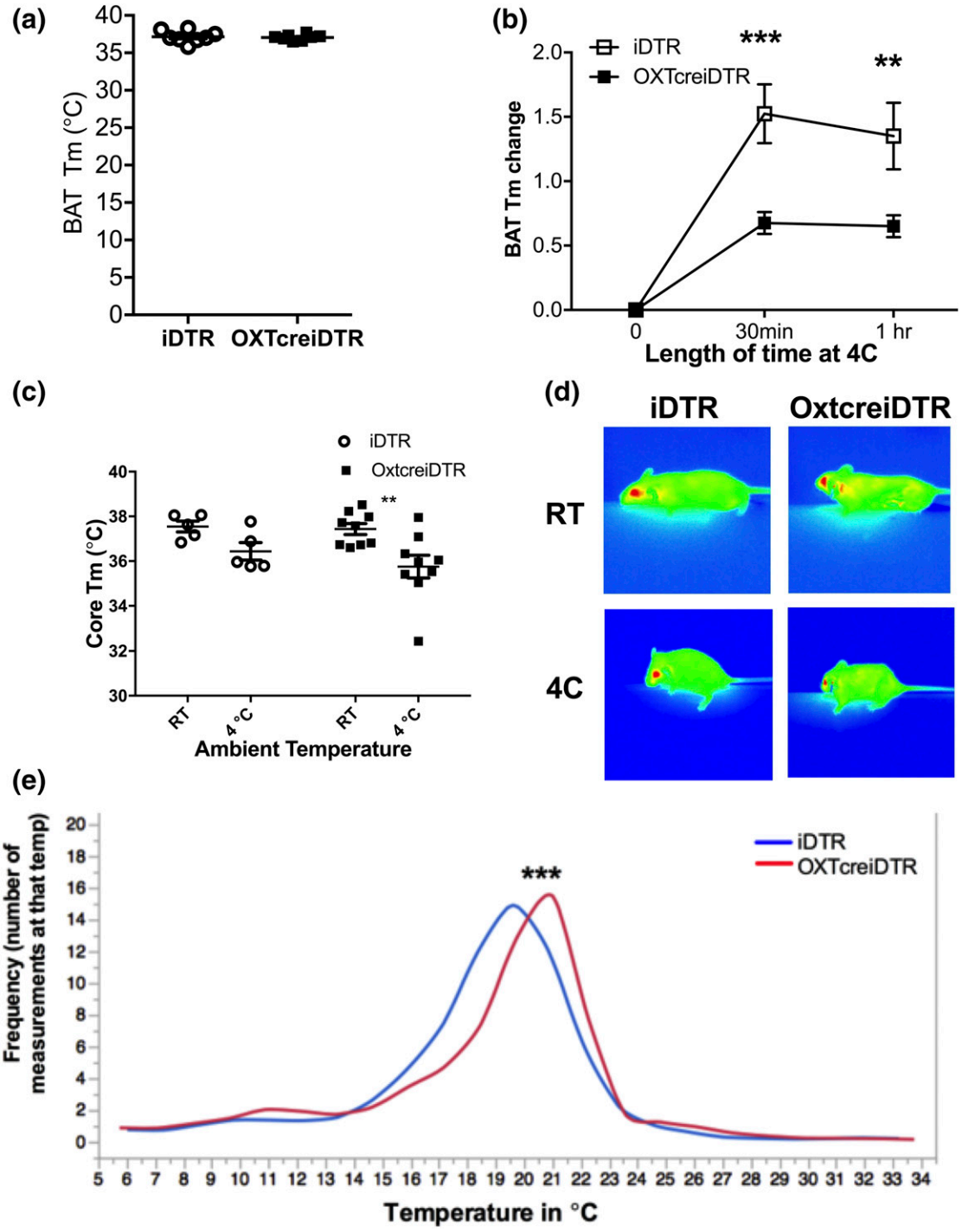

Figure 5. Male OXT-neuron–ablated mice have disrupted thermogenesis. (a) BAT temperature was measured at room temperature. (b) OXTcreiDTR and iDTR mice were placed at 4°C, and BAT temperature change was monitored 30 minutes and 1 hour after cold exposure. (c) Core body temperature was measured at baseline and then at 3 hours. (d) Representative images of thermograph in iDTR and OXTcreiDTR mice at room temperature vs 4°C. (e) Average curves for male skin temperature after 3 hours of cold exposure (difference between group distribution means by Kolmogorov–Smirnov test, $***P < 0.001$; n = 5 for iDTR, n = 4 for OxtiDTC). Red, OxtcreiDTR; blue, iDTR. Error bars indicate standard error of the mean.

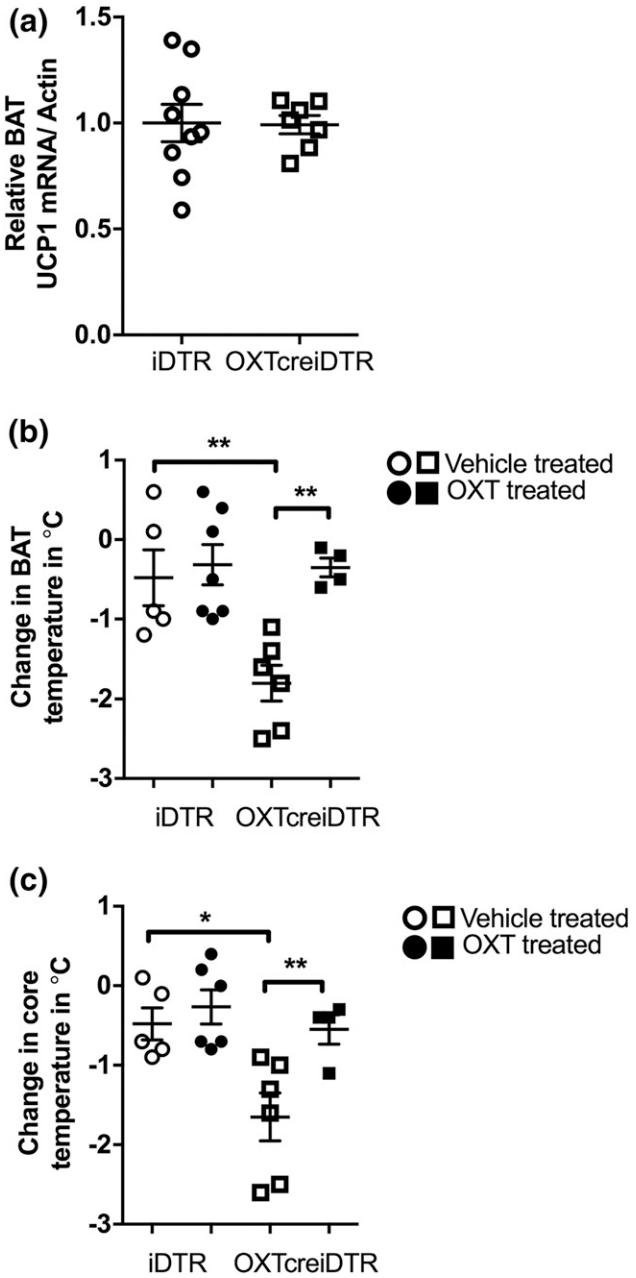

Figure 6. The deficit in cold-induced thermogenesis in male OXT-neuron–ablated mice reflects an acute defect in BAT activation rather than absent BAT capacity. (a) Relative abundance in UCP1 mRNA is not different in OXTcreiDTR and iDTR mice. (b) Oxytocin treatment decreases the cold exposure–mediated temperature drop in the BAT of OXTcreiDTR mice (**$P < 0.01$; n = 6 for each group). (c) Oxytocin treatment decreases the cold exposure–mediated temperature drop in the core temperature of OXTcreiDTR mice (*$P < 0.05$; n = 6 for each group).

Similar to other groups, we used a genetically directed approach to enable the precise targeting of oxytocin neurons [15]. Our initial experiments confirm that our approach caused the specific lesion of oxytocin neurons. As reported, we found that adult lesion of oxytocin-expressing neurons does not alter body weight, food intake, or energy expenditure on chow at room temperature. Thus, our work appears to confirm that OXT neuron ablation, in contrast to pharmacological studies on OXT, did not result in any change of body weight and food intake. It is important to note that negative results for genetic ablation studies may reflect an

incomplete extent of ablation, whereas positive results for pharmacologic studies may reflect a decreased specificity of effect. Similar findings of developmental compensation have been reported with developmental alteration of Agouti-related protein signaling; Agouti-related protein neuron ablation in neonates does not appear to affect body weight and intake, although pharmacological studies predict that Agouti-related protein neuron ablation would alter both of these parameters [24, 25]. These results suggest rapid functional compensation from redundant pathways is sufficient to ameliorate the detrimental effects of neuronal loss at a specific developmental stage.

Consistent with work in oxytocin-knockout mice, we found that adult ablation of oxytocin neurons leads to increased intake of sucrose-containing solution. Although sucrose solution intake is dysregulated in OXT-neuron–ablated mice, their preference for normal chow or high-fat chow remains unchanged. This result raises the intriguing possibility that appetite for high-fat foods may be regulated differently than for carbohydrate-rich liquids. Such a difference in regulation may point toward an explanation for the fact that our body poorly accounts for calories consumed as soda or juice than for calories consumed as high-fat solids.

In recent work, Wu *et al.* [15], using a strategy similar to our approach, found that acute leptin-induced anorexia was diminished in OXT-neuron–ablated mice. Given our understanding that leptin action through OXT-neurons at the PVN is mediated by their effect on CCK-responsive neurons in the NTS, we examined the effect of oxytocin neuron ablation on CCK-induced anorexia. Consistent with our current understanding, oxytocin-ablated mice had a blunted anorexic response to CCK injection coupled with reduced c-fos activity at the level of the PVN, suggesting a loss of forebrain integration of the satiation signal.

In response to cold stress, mice attempt to maintain their body temperature by increasing heat production through BAT thermogenesis [19]. We attempted to examine the hypothesis that oxytocin signaling in the PVN is important in the thermogenic response to cold. Upon exposure to extreme cold, OXT-neuron–ablated mice had a lower core body temperature, lower BAT response to cold and increased heat at the skin. Thus, OXT-neuron–ablated mice had deficits in multiple aspects of temperature homeostasis, namely heat generation as well as heat retention, ultimately leading to a deficit in core body temperature. Based on these results, though the detailed mechanisms for OXT neurons mediating thermogenesis remain unknown, we propose that to adjust the whole body to cold, OXT neurons upregulate BAT function and decrease peripheral vasodilation to reduce energy loss and to maintain body temperature. Central-peripheral neural circuits regulating thermogenesis remain incompletely understood. Environmental or core temperature is sensed and integrated in hypothalamic regions. To evoke behavioral, autonomic, somatic, and hormonal responses that counteract changes in environmental temperature before they affect core body temperature, thermoregulatory command neurons in the POA need to receive feedforward signaling from skin thermoreceptors through spinal and trigeminal dorsal horns. Central thermosensation, mainly by POA neurons, is thought to be an important thermosensory mechanism for body temperature control [26]. The dorsal parvocellular and ventromedial parvocellular divisions of the PVN are a major source of descending projections to sympathetic preganglionic neurons of the intramediolateral nucleus of the spinal cord [27, 28]. OXT neurons provide the largest contribution to this projection [27] and are the greatest number of PVN neurons infected after attenuated pseudorabies virus injections into BAT [29]. Thermogenesis is impaired in OXT and OXT receptor–deficient mice [13, 30] and is restored in OXT receptor–deficient mice by replacement of the OXT receptor in the hypothalamus [31]. Oxytocin knockout mice have reduced sympathetic tone [14].

Although DT treatment significantly decreased the number of OXT neurons in the PVN of OXTcreiDTR mice, AVP, CRH, and TRH neurons were not significantly altered by DT treatment [Fig. 1(c)]. Additionally, OXT-neuron staining was the only subset of neuron staining in the PVN that colocalized with c-fos staining 4 hours after CCK injection (Fig. 4). This suggests that OXT neurons, and not AVP, CRH, or TRH neurons, were in fact responsible for the effects reported in this paper. However, our experiments ablate oxytocin neurons in

both the PVN and SON and cannot exclude a role for the SON in the physiology we describe in this paper.

All of the deficits described here in male OXT-neuron–ablated mice (anorexia in response to CCK, increased consumption of sucrose-containing liquid, and cold-stress related thermogenesis) would seem to predispose to weight gain. Nonetheless, we did not observe weight gain on chow in oxytocin-ablated mice. It may be that a significantly longer observation time at a less thermo-neutral temperature would reveal such a weight change.

Acknowledgments

Address all correspondence to: Jeff Roizen, MD, PhD, Division of Endocrinology, Children's Hospital of Philadelphia, 3401 Civic Center Blvd., Philadelphia, PA 19104. E-mail: jeffroizen@gmail.com.

This work was supported by National Institutes of Health Grant K08-HD087964-01 and by National Center for Research Resources and the National Center for Advancing Translational Sciences, NIH, Grant UL1TR000003. The content is solely the responsibility of the authors and does not necessarily represent the official views of the NIH.

Disclosure Summary: The authors have nothing to disclose.

References and Notes

1. Höybye C, Barkeling B, Espelund U, Petersson M, Thorén M. Peptides associated with hyperphagia in adults with Prader-Willi syndrome before and during GH treatment. *Growth Horm IGF Res*. 2003;**13**(6):322–327.
2. Kublaoui BM, Gemelli T, Tolson KP, Wang Y, Zinn AR. Oxytocin deficiency mediates hyperphagic obesity of Sim1 haploinsufficient mice. *Mol Endocrinol*. 2008;**22**(7):1723–1734.
3. Ludwig M. Dendritic release of vasopressin and oxytocin. *J Neuroendocrinol*. 1998;**10**(12):881–895.
4. Knobloch HS, Charlet A, Hoffmann LC, Eliava M, Khrulev S, Cetin AH, Osten P, Schwarz MK, Seeburg PH, Stoop R, Grinevich V. Evoked axonal oxytocin release in the central amygdala attenuates fear response. *Neuron*. 2012;**73**(3):553–566.
5. Balthasar N, Dalgaard LT, Lee CE, Yu J, Funahashi H, Williams T, Ferreira M, Tang V, McGovern RA, Kenny CD, Christiansen LM, Edelstein E, Choi B, Boss O, Aschkenasi C, Zhang CY, Mountjoy K, Kishi T, Elmquist JK, Lowell BB. Divergence of melanocortin pathways in the control of food intake and energy expenditure. *Cell*. 2005;**123**(3):493–505.
6. Amico JA, Vollmer RR, Cai HM, Miedlar JA, Rinaman L. Enhanced initial and sustained intake of sucrose solution in mice with an oxytocin gene deletion. *Am J Physiol Regul Integr Comp Physiol*. 2005;**289**(6):R1798–R1806.
7. Blevins JE, Schwartz MW, Baskin DG. Evidence that paraventricular nucleus oxytocin neurons link hypothalamic leptin action to caudal brain stem nuclei controlling meal size. *Am J Physiol Regul Integr Comp Physiol*. 2004;**287**(1):R87–R96.
8. Miedlar JA, Rinaman L, Vollmer RR, Amico JA. Oxytocin gene deletion mice overconsume palatable sucrose solution but not palatable lipid emulsions. *Am J Physiol Regul Integr Comp Physiol*. 2007;**293**(3):R1063–R1068.
9. Olszewski PK, Klockars A, Olszewska AM, Fredriksson R, Schiöth HB, Levine AS. Molecular, immunohistochemical, and pharmacological evidence of oxytocin's role as inhibitor of carbohydrate but not fat intake. *Endocrinology*. 2010;**151**(10):4736–4744.
10. Olszewski PK, Klockars A, Schiöth HB, Levine AS. Oxytocin as feeding inhibitor: maintaining homeostasis in consummatory behavior. *Pharmacol Biochem Behav*. 2010;**97**(1):47–54.
11. Sclafani A, Rinaman L, Vollmer RR, Amico JA. Oxytocin knockout mice demonstrate enhanced intake of sweet and nonsweet carbohydrate solutions. *Am J Physiol Regul Integr Comp Physiol*. 2007;**292**(5):R1828–R1833.
12. Blevins JE, Eakin TJ, Murphy JA, Schwartz MW, Baskin DG. Oxytocin innervation of caudal brainstem nuclei activated by cholecystokinin. *Brain Res*. 2003;**993**(1-2):30–41.
13. Takayanagi Y, Kasahara Y, Onaka T, Takahashi N, Kawada T, Nishimori K. Oxytocin receptor-deficient mice developed late-onset obesity. *Neuroreport*. 2008;**19**(9):951–955.
14. Camerino C. Low sympathetic tone and obese phenotype in oxytocin-deficient mice. *Obesity (Silver Spring)*. 2009;**17**(5):980–984.

15. Wu Z, Xu Y, Zhu Y, Sutton AK, Zhao R, Lowell BB, Olson DP, Tong Q. An obligate role of oxytocin neurons in diet induced energy expenditure. *PLoS One*. 2012;**7**(9):e45167.
16. Morton GJ, Thatcher BS, Reidelberger RD, Ogimoto K, Wolden-Hanson T, Baskin DG, Schwartz MW, Blevins JE. Peripheral oxytocin suppresses food intake and causes weight loss in diet-induced obese rats. *Am J Physiol Endocrinol Metab*. 2012;**302**(1):E134–E144.
17. Bachman ES, Dhillon H, Zhang CY, Cinti S, Bianco AC, Kobilka BK, Lowell BB. betaAR signaling required for diet-induced thermogenesis and obesity resistance. *Science*. 2002;**297**(5582):843–845.
18. Ueta CB, Fernandes GW, Capelo LP, Fonseca TL, Maculan FD, Gouveia CH, Brum PC, Christoffolete MA, Aoki MS, Lancellotti CL, Kim B, Bianco AC, Ribeiro MO. β(1) Adrenergic receptor is key to cold- and diet-induced thermogenesis in mice. *J Endocrinol*. 2012;**214**(3):359–365.
19. Yoshida K, Li X, Cano G, Lazarus M, Saper CB. Parallel preoptic pathways for thermoregulation. *J Neurosci*. 2009;**29**(38):11954–11964.
20. Peterson CM, Lecoultre V, Frost EA, Simmons J, Redman LM, Ravussin E. The thermogenic responses to overfeeding and cold are differentially regulated. *Obesity (Silver Spring)*. 2016;**24**:96–101.
21. Xi D, Gandhi N, Lai M, Kublaoui BM. Ablation of Sim1 neurons causes obesity through hyperphagia and reduced energy expenditure. *PLoS One*. 2012;**7**(4):e36453.
22. Altirriba J, Poher AL, Caillon A, Arsenijevic D, Veyrat-Durebex C, Lyautey J, Dulloo A, Rohner-Jeanrenaud F. Divergent effects of oxytocin treatment of obese diabetic mice on adiposity and diabetes. *Endocrinology*. 2014;**155**(11):4189–4201.
23. Billings LB, Spero JA, Vollmer RR, Amico JA. Oxytocin null mice ingest enhanced amounts of sweet solutions during light and dark cycles and during repeated shaker stress. *Behav Brain Res*. 2006;**171**(1): 134–141.
24. Wu Q, Howell MP, Cowley MA, Palmiter RD. Starvation after AgRP neuron ablation is independent of melanocortin signaling. *Proc Natl Acad Sci USA*. 2008;**105**(7):2687–2692.
25. Luquet S, Perez FA, Hnasko TS, Palmiter RD. NPY/AgRP neurons are essential for feeding in adult mice but can be ablated in neonates. *Science*. 2005;**310**(5748):683–685.
26. Nakamura K, Morrison SF. Central efferent pathways mediating skin cooling-evoked sympathetic thermogenesis in brown adipose tissue. *Am J Physiol Regul Integr Comp Physiol*. 2007;**292**(1): R127–R136.
27. Sawchenko PE, Swanson LW. Immunohistochemical identification of neurons in the paraventricular nucleus of the hypothalamus that project to the medulla or to the spinal cord in the rat. *J Comp Neurol*. 1982;**205**(3):260–272.
28. Swanson LW, Sawchenko PE. Hypothalamic integration: organization of the paraventricular and supraoptic nuclei. *Annu Rev Neurosci*. 1983;**6**:269–324.
29. Oldfield BJ, Giles ME, Watson A, Anderson C, Colvill LM, McKinley MJ. The neurochemical characterisation of hypothalamic pathways projecting polysynaptically to brown adipose tissue in the rat. *Neuroscience*. 2002;**110**(3):515–526.
30. Kasahara Y, Takayanagi Y, Kawada T, Itoi K, Nishimori K. Impaired thermoregulatory ability of oxytocin-deficient mice during cold-exposure. *Biosci Biotechnol Biochem*. 2007;**71**(12):3122–3126.
31. Kasahara Y, Sato K, Takayanagi Y, Mizukami H, Ozawa K, Hidema S, So KH, Kawada T, Inoue N, Ikeda I, Roh SG, Itoi K, Nishimori K. Oxytocin receptor in the hypothalamus is sufficient to rescue normal thermoregulatory function in male oxytocin receptor knockout mice. *Endocrinology*. 2013; **154**(11):4305–4315.